COBEM 2023 27TH INTERNATIONAL CONGRESS OF MECHANICAL ENGENEERING

ABCM Brazilian Society of Mechanical Sciences and Engineering
27th ABCM International Congress of Mechanical Engineering
December 04-08, 2023, Florianópolis-SC, Brazil

COB-2023-0962
RESIDUAL STRESS IN ADDITIVE MANUFACTURED POLYMERS

Arthur Adeodato
Departamento de Engenharia Mecânica, Instituto Politécnico, Universidade do Estado do Rio de Janeiro, UERJ – Rua Bonfim 25, Nova Friburgo, RJ, Brasil.
arthuradeodato@iprj.uerj.br

Yago Chagas Santos Santiago
CEFET/RJ, Estr. de Adrianópolis, 1317 - Vila Nossa Sra. da Conceição, Nova Iguaçu, RJ, Brazil.
yago.moura@aluno.cefet-rj.br

Lucas Lisboa Vignoli
Center for Technology and Application of Composite Materials, Department of Mechanical Engineering, Federal University of Rio de Janeiro, Macaé, RJ, Brazil.
ll.vignoli@mecanica.coppe.ufrj.br

Daniel de Macedo Barreto Netto
Brenno Tavares Duarte
Paulo Pedro Kenedi
Programa de Pós-Graduação em Engenharia Mecânica e Tecnologia de Materiais, PPEMM, CEFET/RJ,
Rua Maracanã, 229, RJ, Brasil.
daniel.netto@aluno.cefet-rj.br, brenno.duarte@cefet-rj.br, paulo.kenedi@cefet-rj.br

Abstract. *Additive manufacturing (AM) is a technological advancement that has significantly transformed the manufacturing industry by enabling the production of complex geometries with high precision and accuracy. This technology has found numerous applications in various fields, including aerospace, automotive, biomedical, and consumer products. However, it has been observed that internal stresses, which refer to the residual stresses, that remain in the material after printing and solidification, can significantly affect the mechanical response and reliability of the printed components. This fact can lead to unpredictable behaviors and premature damage issues. This paper aims to investigate the effects of residual stresses on the mechanical behavior of polymer-based materials, specifically poly-lactic acid (PLA) and PLA with carbon particles (PLACP). Different specimens are printed and tested in a universal material test machine, for mechanical characterization. The residual stresses are indirectly evaluated through the utilization of the slitting method. A comparison between PLA with and without carbon particles is performed to gain an insight into which combination of characteristics of the AM process is favorable to minimize the presence of the specimen's residual stress. The results can contribute to the ongoing efforts to address the challenges associated with AM and the advances in this technology.*

Keywords: *residual stress, additive manufacturing, polymer characterization, experimental procedures.*

1. INTRODUCTION

The fabrication processes of components have been significantly improved over the last decades with the advent of additive manufacturing (AM) technology, Valvez et al. (2020). This method has revolutionized the manufacturing industry by allowing fast speed in manufacturing, especially for complex geometries, Daminabo et al. (2020). In parallel, the development of polymers has opened new options for the manufacturing industry due to their unique properties such as low density, high toughness, and excellent chemical resistance, Dizon et al. (2018). Polymers have been successfully utilized in a variety of industrial applications such as automotive, Friedrich et al. (2013), aerospace, Martinez et al. (2022), and biomedical industries, Vanaei et al. (2021). The use of polymer-based materials has enabled the development of lightweight and efficient products, leading to significant cost savings and improved performance.

The AM polymer's 3D printing process still presents several challenges that can affect the quality and durability of the final product. Warping, layer adhesion, dimensional accuracy, and post-processing effects are some of the main challenges faced in this field, Xie et al. (2022). Another critical issue is the residual stresses introduced during the AM process that can significantly affect the mechanical properties and reliability of the printed parts. Residual stresses, that remain in the material after the printing process has ended, are even more pronounced in polymer-based materials than in metal ones. Residual stresses can arise due to a range of factors including severe thermal gradients, high curing

shrinkage, and layer-by-layer deposition when compared to metal materials, Li et al. (2018). The thermal gradient, the temperature difference that occurs between different regions of a printed object during the printing process, can be responsible for significant changes in the mechanical properties of the printed parts, Hsueh et al. (2021). The material rapid heating and cooling during printing can lead to non-uniform thermal expansion and contraction, resulting in residual stresses that can affect the structural integrity and performance of the printed component, Samy et al. (2021).

To mitigate the effects of thermal gradients, it is essential to control the energy source's intensity and deposition duration to ensure uniform melting and solidification of the material, Das et al. (2020). Additionally, the use of heated build platforms and cooling systems can help regulate the temperature distribution during printing and reduce the thermal gradient, Abas et al. (2022). Optimizing the printing parameters, such as the layer thickness, print speed, and orientation, can help minimize thermal gradients and improve the mechanical properties of the printed parts. Curing shrinkage is another critical phenomenon that occurs during the additive manufacturing (AM) process, especially for polymer-based materials. It is a volumetric shrinkageof the material that occurs during the solidification or curing process. The effects of curing shrinkage can be attenuated by controlling the temperature and humidity during the curing process, improving the dimensional accuracy of the printed part. Moreover, post-processing techniques, such as annealing or stress relief, can be applied to reduce the residual stresses and improve the mechanical properties of the printed part, Oliaei et al. (2016).

Several efforts have been made to measure, or even to estimate the residual stress induced by the printing process. According to Lu (1996), it is only possible to measure residual stresses indirectly. The principle of indirect estimation of residual stress relies on the measurement of strain or deflection that happens because of the rebalancing of internal stresses. Hence, destructive, and non-destructive techniques can be employed for this purpose. Hole drilling, layer removal, ring core, and slitting method can be employed to achieve this condition, Rossini et al. (2012) and Schajer et al. (2013). The resultant strains or deflections can be measured, for instance, by strain gauges, Rendler et al. (1996), or by digital image correlation, Bartlett et al. (2018). Also, stress relief may be estimated by analytical solutions or even using numerical approaches, such as the finite element method. Regarding polymers, Liu et al. (2019) provide an extensive review comparing pure PLA with PLACP (polymer-based carbon particles) highlighting the difference in mechanical proprieties between them. Xinhua et al. (2015) investigated the distortion in PLA thin plates, through a model based on elasticity and thermoelasticity theories. A total of 81 specimens were printed and measured with a portable 3D laser scanner. The authors used Raman spectroscopy to evaluate the residual stresses developed on the surface of the sample and correlate it with stress concentration due to the unavoidable porous formation. Recently, Zhu et al. (2022) investigated a feedback control during the fusing process deposition of PLA samples for the minimization of residual stresses. The results suggested that the residual stress decreases with increasing layer thickness, printing speed, and platform temperature. As a result, the authors concluded that it is possible to minimize the printed error by augmenting the nozzle temperature.

Post-processing techniques have been developed to improve the mechanical properties and reliability of the printed parts. The alternatives to minimize residual stresses in printed polymers rely on experimental approaches during the printing process or as a post-procedure. Alsoufi et al. (2019) experimentally investigated the influence of nozzle temperature on the mechanical properties of PLA and PLACP 20%. The phenomenon of warping, dimensional distortion, and density changes was detected. Specimens of 63.5 x 9.53 x 3.2 mm were printed for 195 to 250 °C with 5 °C increments and infill directions of 0°, 90°, 45° and ± 45°. Jayanth et al. (2021) noted a notorious improvement in the mechanical properties of PLA-printed parts submitted to heat treatment. It is attributed to a significant reduction in the internal stresses developed during the printing process. An annealing of 100° C for 4 hours is possible to enhance 80% in PLA tensile strength. This treatment can be used as a post-processing for minimizing residual stresses.

In this paper, the effects of residual stress on the mechanical properties of PLA and PLACP specimens are preliminarily investigated through the slitting method. The objective is to compare the PLA and PLACP specimen's performance regarding the indirect measurement of the specimen's dimensional distortion, using the back face strain gages. The mechanical characterization of PLA and PLACP materials was implemented through the measurement of mechanical properties such as elastic modulus, yielding limit, and rupture strain. PLA and PLACP specimens were milled in the slitting method, to promote sequential stress relief with the strains measured by a back-faced strain gage. The findings of this study provide preliminary insights into the design and manufacturing of polymer-based AM parts for a wide range of applications.

2. MATERIAL AND METHODS

This section is dedicated to exposing the materials and experimental setup employed to investigate indirectly the residual stress promoted during the additive manufacturing process of polymers. Tensile tests are performed for mechanical characterization while the slitting method is employed for residual stress investigation.

2.1 Mechanical characterization

The mechanical characterization analysis is performed to obtain the necessary parameters of the materials involved, such as elastic modulus, yielding limit, and rupture strain. For this purpose, specimens of each material are submitted to axial tensile tests as shown in Figure 1.a. The stress-strain curves are built by using an Instron testing system (5966 model) with a controlled displacement rate of 10 mm/min and the strain signal is captured by a clip gauge.

(a) (b)

Figure 1. Experimental apparatus for PLA and PLACP tests: (a) Tensile and (b) Residual stress.

Figure 2 shows the output of the Instron testing system for the set of four specimens of PLA and PLACP.

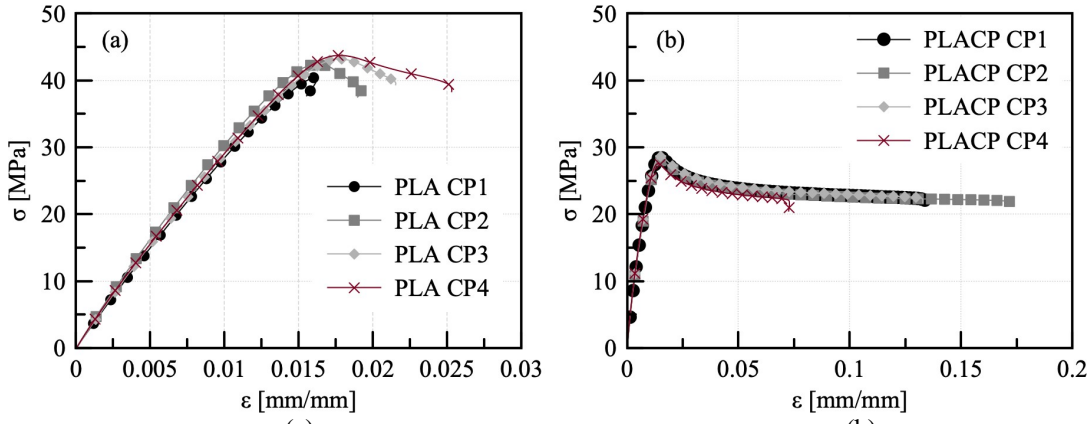

(a) (b)

Figure 2. Stress vs strain diagram from tensile tests of (a) PLA and (b) PLACP.

PLA specimens present a larger yielding limit S_y than PLACP specimens, but a smaller rupture strain ε_r. Table 1 shows the quantitative values obtained from the tensile tests presented in Figure 2.

Table 1. PLA and PLACP mechanical properties.

	E(GPa)		S_y (MPa)		ε_r (m/m)	
	PLA	PLACP	PLA	PLACP	PLA	PLACP
CP1	2.8	2.2	40.4	28.5	0.016	0.13
CP2	3.0	2.1	42.2	28.0	0.019	0.17
CP3	2.9	2.2	43.1	28.6	0.021	0.13
CP4	2.8	2.2	43.7	27.5	0.025	0.07
Average	2.9	2.2	42.4	28.2	0.020	0.013

Note that the elastic modulus E of both materials is quite similar. The PLA specimens presented an overall more fragile behavior if compared with PLACP specimens.

2.2 Experimental Setup

The specimens are printed in a 3D plotter (Ender 6 from Creality) and two different polymeric materials were used: PLA, and PLACP. The specimens were printed using a slit height of 0.2 mm, 3 walls of 0.8 mm thickness, 100% of infill, with 60°C of bed temperature, and print cooling enabled at 100% of fan speed. As the pieces are flat-bottomed, no supports were required, and the PLA specimens were made at a hot-end printing temperature of 190°C and a print speed of 120 mm/s, while PLACP specimens were made at a temperature of 210°C and a print speed of 60 mm/s. The experimental setup for the residual stress investigation is shown in Figure 1. b and is composed of a milling machine NMF144R from *Nagano* with a 6 mm bit rotating at 2000 rpm.

The specimens are in geometric and dimensional agreement with standard ISO 1690. The specimens are printed in rectangular prism shapes with 10 x 10 x 45 mm. Strain gage from Excel Sensores, in a quarter bridge configuration, of 120 Ω resistance, is bonded with cyanoacrylate at the specimen back face, as shown in Figure 4. b Afterwards, each specimen is coupled to the milling machine, and the slitting method is employed removing 0.2 mm per slit, from as printed specimen top face through its original neutral line position. A *Spider* 600 Hz HBM was used as data acquisition hardware, in conjunction with HBM Catman software, to capture the strain gage signals.

2.3. Analytical model

The analytical model handles the conversion between the strains measured by the back-faced strain gage, during the sequential removal of material by the slitting method, to the respective moment relief.

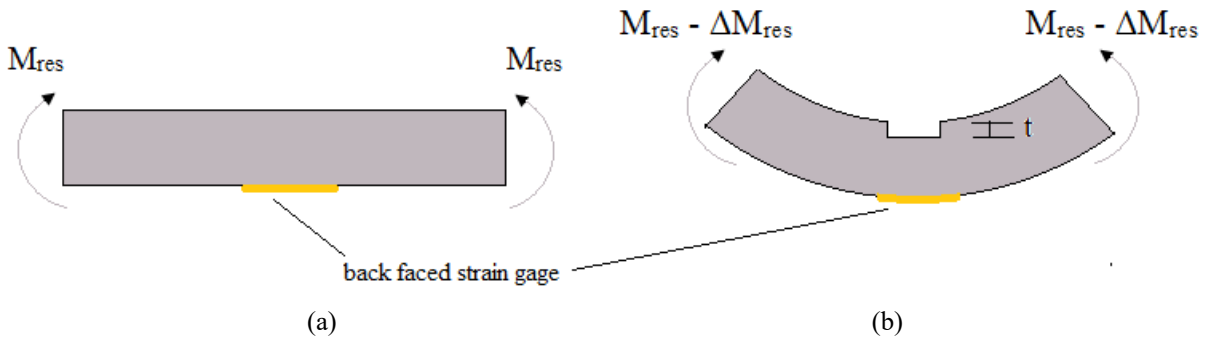

Figure 3. Slitting method sequence. (a) specimen as printed and (b) specimen with one slit.

Note that in Figure 3.a, the specimen, as printed, has an initial state of built-in residual stress distribution. M_{res} represents the initial residual bending moment. Note that although the residual stress can change in function of the cross-section's vertical position, the residual bending moment has only one value for the entire cross-section. The strain gage is attached after the print has ended, so the strain that is acting on the strain gage, at the moment represented by Figure 3. a, is null. Equation (1) was developed through the utilization of the solid mechanics theory. It assumes that the initial specimen cross-section is a square, and as the specimen has slits being milled, the moment of inertia of the area diminishes progressively.

$$\Delta M_{res}(\Delta\varepsilon_n) = \frac{2}{3} \cdot b \cdot \left(c - n \cdot \frac{t}{2}\right)^2 \cdot E \cdot \Delta\varepsilon_n \quad (1)$$

ΔM_{res} is the bending moment relief caused by the removal of one slit, $\Delta\varepsilon_n$ is the strain relief caused by the removal of one slit, b is the width and c is the semi-height of the specimen cross-section, n is the number of the slit and t is the slit height (in this work it is used 0.2 mm).

3. RESULTS

Figure 4.a shows a PLA specimen after has been milled, in the slitting method, up to the original neutral line position. Figure 3. b shows the strain gage attached to the specimen's back face.

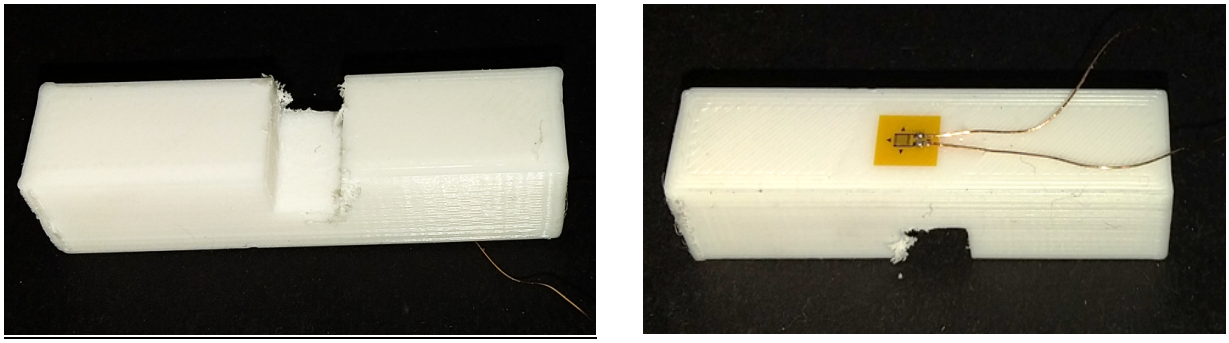

(a) (b)

Figure 4. PLA specimen: (a) After the slitting method has ended and (b) strain gage attached at the specimen's back face.

Figure 5. a shows the graphical representation of the strains registered during the slitting method test applied to PLA and PLACP specimens. Figure 5. b shows the strain results of central portions of Figure 5. a converted to bending moment relief, using Eq. (1), caused by the removal of slits.

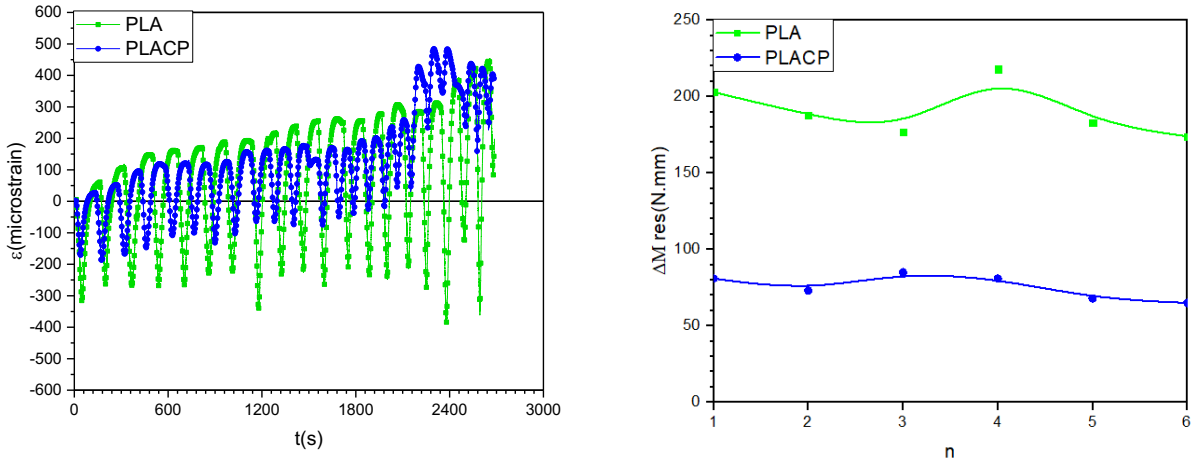

(a) (b)

Figure 5. Graphical representation of the Slitting method tests for PLA and PLACP specimens: (a) strains and (b) bending moment relief.

In a few words, Figure 5. a can be divided into two phases: in the first phase the strains go from the peak to the valley, when the milling cutter is active; and in the second phase the strains go from the valley to the peak, when the milling cutter is not active, and the specimen is bending for a new equilibrium position.

Twelve second phase $\Delta\varepsilon_n$ signals (obtained between 600 and 1620 s), after being converted in ΔM_{res} through the utilization of Eq. (1), are used in Figure 5.b: six for PLA specimen and six for PLACP specimen. Note that the PLA specimen shows almost double the bending moment relief caused by slit removal than the PLACP specimen. Also, the values varied much more in the PLA specimen than in the PLACP specimen. The values of ΔM_{res}, used in Figure 5.b, are disponible in Table 2.

Table 2. PLA and PLACP slitting method results.

n	$\Delta\varepsilon_n$(μstrain)		$\Delta M_{res}(\Delta\varepsilon_n)$ N·mm	
	PLA	PLACP	PLA	PLACP
1	438	231	203	81
2	422	217	188	73
3	414	261	177	85
4	534	261	218	81
5	467	228	183	68
6	465	230	174	65

Note that for both values of $\Delta\varepsilon_n$ and ΔM_{res}, the PLA specimen results has almost the double of the values of the PLACP specimen results. These results configure that the PLACP specimen has a much better performance since generates less ΔM_{res} per slit than PLA specimen.

4. CONCLUSIONS

Additive manufacturing, commonly referred to as 3D printing, is an innovative and rapidly evolving technology that offers several advantages over traditional manufacturing techniques. However, the printing process can be significantly altered by several phenomena such as thermal gradient and curing shrinkage, which can result in the development of residual stress in the final printed product. This paper investigated, in a comparative way, the residual stress consequence, in terms of bending moment relief, caused by sequential slit removal. For PLA and PLACP specimens tested, as described in subsection 2.2; the PLACP specimen presented a less important bending moment relief caused by slit removal in comparison with the PLA specimen. These points out that parts fabricated with PLACP material would have a minor warping and dimensional distortion in comparison with the ones fabricated with PLA material.

5. ACKNOWLEDGMENTS

The authors would like to acknowledge the support of the Brazilian Research Agencies CNPq, FAPERJ, and CAPES.

6. REFERENCES

Abas, M., Habib, T., Noor, S., Salah, B., and Zimon, D., 2022, Parametric investigation and optimization to study the effect of process parameters on the dimensional deviation of fused deposition modeling of 3D printed parts, *Polymers*, Vol. 14(17), pp.3667. https://doi.org/10.3390/polym14173667.

Alsoufi, M.S., Alhazmi, M.W., Suker, D.K., Alghamdi, T.A., Sabbagh, R.A., Felemban, M.A. and Bazuhair, F.K., 2019, Experimental characterization of the influence of nozzle temperature in fdm 3D printed pure PLA and advanced PLA+, American Journal of Mechanical Engineering, Vol. 7(2), pp.45–60. https://drive.uqu.edu.sa/ /usj/files/Dr MohammadAlsoufi/ajme-7-2-1.pdf.

Bartlett, J.L. Croom, B.P., Burdick, J., H enkel, D., and Li, X., 2018, Revealing mechanisms of residual stress development in additive manufacturing via digital image correlation, Additive Manufacturing, Vol. 22, pp.1–12, ISSN 2214-8604. https://doi.org/10.1016/j.addma.2018.04.025.

Daminabo, S.C., Goel, S., Grammatikos, S.A., Nezhad, H.Y., and Thakur, V.K., 2020, Fused deposition modeling-based additive manufacturing (3D printing): techniques for polymer material systems, Materials Today Chemistry, Vol. 16, pp.100248, ISSN 2468-5194. https://doi.org/10.1016/j.mtchem.2020.100248.

Das, A., Chatham, C.A., Fallon, J.J., Zawaski, C.E., Gilmer, E.L., Williams, C.B. and Bortner, M.J., 2020. Current understanding and challenges in high-temperature additive manufacturing of engineering thermoplastic polymers, Additive Manufacturing, Vol. 34, pp.101218, ISSN 2214-8604. https://doi.org/10.1016/j.addma.2020. 101218.

Dizon, J.R.C., Espera Jr, A.H., Qiyi, C. and Rigoberto, C.A., 2018, Mechanical characterization of 3D-printed polymers, Additive manufacturing, Vol. 20, pp. 44–67. https://doi.org/10.1016/j.addma.2017.12.002.

Friedrich, K. and Almajid, A.A., 2013, Manufacturing aspects of advanced polymer composites for automotive applications, Applied Composite Materials, Vol. 20, pp. 107–128, https://doi.org/10.1007/s10443-012-9258-7.

Hsueh, M., Lai, C., Wang, S., Zeng, Y., Hsieh, C., Pan, C. and Huang, W., 2021, Effect of printing parameters on the thermal and mechanical properties of 3D-printed PLA and PETG, using fused deposition modeling, Polymers, Vol. 13 (11), pp. 1758. https://doi.org/10.3390/polym13111758.

Jayanth, N., Jaswanthraj, K., Sandeep, S., Mallaya, N.H. and Siddharth, S.R., 2021, Effect of heat treatment on mechanical properties of 3D printed PLA, Journal of the Mechanical Behavior of Biomedical Materials, Vol. 123, pp.104764, ISSN 1751-6161. https://doi.org/10.1016/j.jmbbm.2021.104764.

Li, H. Wang, T., Li, Q., Yu, Z. and Wang, N., 2018, A quantitative investigation of distortion of polylactic acid/PLA part in FDM from the point of interface residual stress, The International Journal of Advanced Manufacturing Technology, Vol. 94, pp. 381–395. https://doi.org/10.1007/s00170-017-0820-1.

Liu, Z., Wang, Y., Wu, B., Cui, C., Guo, Y. and Yan, C., 2019, A critical review of fused deposition modeling 3D printing technology in manufacturing polylactic acid parts, The International Journal of Advanced Manufacturing Technology, Vol. 102, pp. 2877–2889.https://doi.org/10.1007/s00170-019-03332-x.

Lu, J. 1996. *Handbook of Measurement of Residual Stresses*. Fairmont Press, Society of Experimental Mechanics, USA.

Martinez, D.W. Espino, M.T., Cascolan, H.M., Crisostomo, J.L. and Dizon, J.R.C., 2022, A comprehensive review of the application of 3D printing in the aerospace industry, Key Engineering Materials, Vol. 913, pp.27–34. https://doi.org/10. 4028/p-94a9zb.

Oliaei, E., Heidari, B.S., Davachi, S.M., Bahrami,M., Davoodi, S., Hejazi, I. and Seyfi, J., 2016, Warpage and shrinkage optimization of injection-molded plastic spoon parts for biodegradable polymers using Taguchi,

ANOVA, and artificial neural network methods, Journal of Materials Science & Technology, Vol. 32(8), pp. 710– 720, ISSN 1005-0302. https://doi.org/10.1016/j.jmst.2016.05.010.

Rendler, N.J. and Vigness, I., 1966, Hole-drilling strain-gage method of measuring residual stresses: authors indicate that this method permits the magnitudes and principal directionsof residual stresses at the hole location to be determined, Experimental Mechanics, Vol. 6, pp. 577–586. https://doi.org/10.1007/BF02326825.

Rossini, N.S., Dassisti, M., Benyounis, K.Y. and Olabi, A., 2012, Methods of measuring residual stresses in components, Materials & Design, Vol. 35, pp.572–588. https://doi.org/10.1016/j.matdes.2011.08.022.

Samy, A. Golbang, A., Harkin-Jones, E., Archer, H.E., Tormey, D. and McIlhagger, A., 2021, Finite element analysis of residual stress and warpage in a 3D printed semi-crystalline polymer: Effect of ambient temperature and nozzle speed, Journal of Manufacturing Processes, Vol. 70, pp.389–399, ISSN 1526-6125. https://doi.org/10.1016/j.jmapro.2021.08.054.

Schajer, G.S. and Ruud, C.O., 2013, Overview of residual stresses and their measurement, Practical residual stress measurement methods, pp. 1–27. https://doi.org/10.1002/9781118402832.ch1.

Valvez, S., Santos, P., Parente, J.M., Silva, M.P. and Reis, P.N.B., 2020, 3D printed continuous carbon fiber reinforced PLA composites: A short review, Procedia Structural Integrity, Vol. 25, pp. 394–399, ISSN 2452-3216. https://doi.org/10.1016/j.prostr.2020.04.056. 1st Virtual Conference on Structural Integrity - VCSI1.

Vanaei, S., Parizi, M.S., Vanaei, S., Salemizadehparizi, F. and Vanaei, H.R., 2021, An overview of materials and techniques in 3D bioprinting toward biomedical application, Engineered Regeneration, Vol. 2, pp.1–18, ISSN 2666-1381. https://doi.org/10.1016/j.engreg.2020.12.001.

Xie, D., Lv, F., Yang, Y., Shen, L., Tian, Z., Shuai, C., Chen, B., and Zhao, J., 2022, A review on distortion and residual stress in additive manufacturing, Chinese Journal of Mechanical Engineering: Additive Manufacturing Frontiers, Vol. 1(3), pp.100039, ISSN 2772-6657. https://doi.org/10.1016/j.cjmeam.2022.100039.

Xinhua, L., Shengpeng, L., Zhou, L., Xianhua, Z., Xiaohu, C. and Zhongbin, W., 2015, An investigation on distortion of PLA thin-plate part in the FDM process, The International Journal of Advanced Manufacturing Technology, Vol. 79, pp. 1117–1126. https://doi.org/10.1007/s00170-015-6893-9.

Zhu, Q., Yu, K., Li, H., Zhang, Q. and Tu, D., 2022, Rapid residual stress prediction and feedback control during fused deposition modeling of PLA, The InternationalJournal of Advanced Manufacturing Technology, pp.1–12. https://doi.org/10.1007/s00170-021-08158-0.

7. RESPONSIBILITY NOTICE

The authors are the only responsible for the printed material included in this paper.